

Research Article

Wide-Band High-Gain DGS Antenna System for Indoor Robot Positioning

Lu Bai  and Chenglie Du

School of Computer Science and Engineering, Northwestern Polytechnical University, Xi'an 710072, China

Correspondence should be addressed to Lu Bai; bailu614@mail.nwpu.edu.cn

Received 15 June 2018; Revised 20 August 2018; Accepted 10 September 2018; Published 20 January 2019

Academic Editor: Xiulong Bao

Copyright © 2019 Lu Bai and Chenglie Du. This is an open access article distributed under the Creative Commons Attribution License, which permits unrestricted use, distribution, and reproduction in any medium, provided the original work is properly cited.

Based on multisource wireless signal fusion technology, the autonomous positioning systems of robots have been widely employed. How to design a compact composable antenna array for indoor robot positioning is still a problem. In this study, we proposed a compact ultrathin antenna unit that effectively reduces the mutual coupling between any adjacent units, while covering most of the existing communication bands, including 2G/3G/4G/Wi-Fi, which will greatly reduce the size of the positioning antenna array. The proposed antenna system has been employed for positioning purpose with high-gain, wide-frequency band and limited size. It necessarily improves the accuracy of positioning signal from various unknown sources and finally accomplishes its autonomous positioning function.

1. Introduction

In the last few years, with the rapid development of the economy, science, and technology, intelligent robots have emerged in every aspect of work and life. Multiple disciplines related to the robot systems, e.g., sensors, data conversion, signal processing and control, artificial intelligence, and bionics, have made remarkable achievements. However, robot positioning, especially in complex environments, remains an unsolved problem [1]. In any indeterminate environment, a robot would scan the surroundings and creates an environmental floor plan for navigation. After an instruction is received, the robot retrieves correlation data of the target to seek the best route and achieve an autonomous cruising task. However, the most important prerequisite of robot precision autonomous positioning is to establish a high-precision route database and ensure cruise accuracy [2]. Presently, normal positioning systems include laser ranging sensors, RFID identification sensors, inertial navigation systems (e.g., gyroscopes and accelerometers), the raster map technology, etc. [3–6].

In this study, we propose a comprehensive positioning RF device by using various existing communication signals.

By transmitting and receiving any 2G/3G/4G/Wi-Fi signal, the novel wireless RF device would obtain real-time high-accuracy positioning data through a positioning algorithm. When a robot is employed in an unknown environment, it will scan all nearby wireless signal sources and obtain connections with them. With the robot cruising the work area and drawing a blueprint, the positioning system also collects the various wireless signals and makes precise area location within its coverage region. In this way, the robot needs a compact antenna system which can cover more communication standards and receive weak signals from different directions. This means that the positioning antenna system needs small size, high-gain multiband.

However, in present, as multi/ultrawide-band high-gain positioning antennas are usually bulky, it is difficult to be installing on small robots. Therefore, a miniaturized robot positioning antenna unit is urgently needed [7–9]. In order to accurately detect the positioning signal source within its coverage region, the proposed positioning antenna system also requires wide-frequency band and good directionality. In this study, we propose an ultrasmall antenna unit and its array that provide small size, broad-frequency band, diverse layout, and

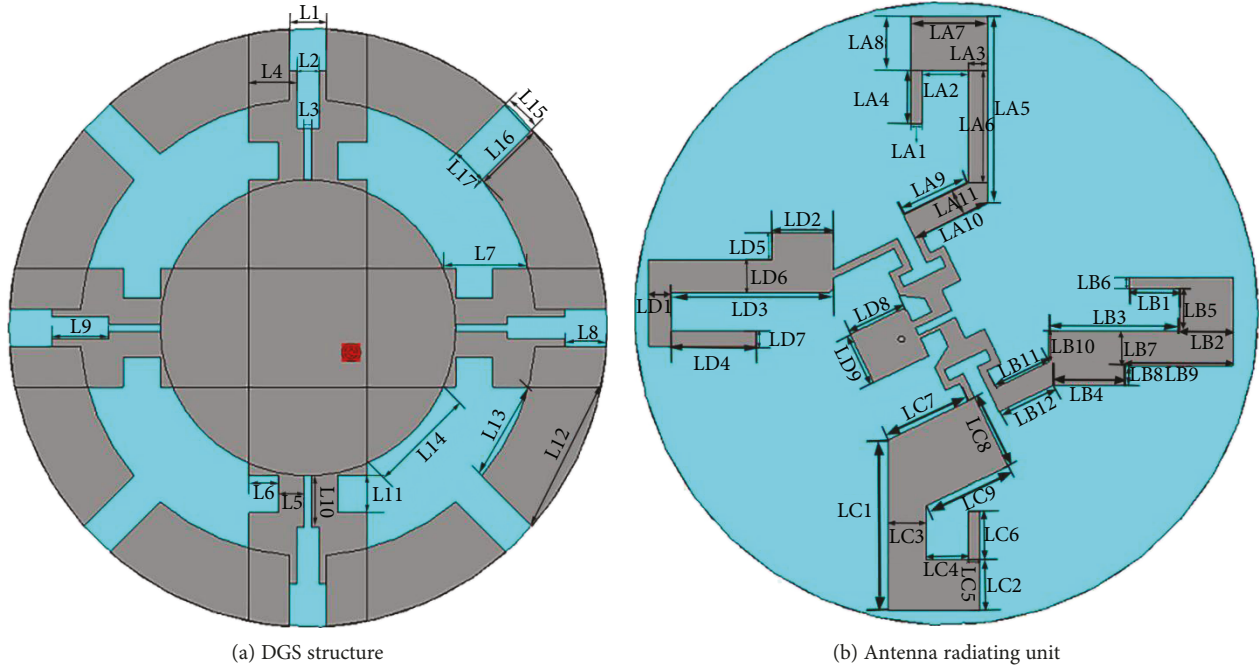


FIGURE 1: DGS antenna unit.

Omni-directional coverage to high-precision positioning systems of small mobile robots.

2. Design Ideas and Methods

For an indoor robot, to collect high-precision wireless signal and obtain accurate positioning data, one small-sized high-precision wireless positioning antenna system is proposed in this paper. The most important for a robot positioning antenna is to reduce the size of antenna; some references [10–12] have proposed various methods to reduce the size of the antenna radiating unit below one-fourth the wavelength, such as a low-profile dual-polarized antenna, an EBG structure antenna as radiating element, or a high-impedance periodic metal structure.

Here, one periodic defected ground structure (DGS) as the antenna reflector plate is proposed to improve antenna gain and reduce the size of position antenna. DGS, an etched periodic or nonperiodic cascaded configuration defect in ground of a planar transmission line (which disturbs the shield current distribution in the ground plane cause of the defect in the ground), is intentionally modified to enhance performance [13–17]. According to the literature [18], in order to obtain a compact broadband antenna, one optimized DGS has been integrated with the antenna radiating unit. Based on this principle, some specific aerial elements and reflecting DGS have been employed; the antenna unit is printed on either side is a dielectric substrate with relative permittivity of 4.4 and 1 mm thickness. The robot RF position modularity requires higher gain, smaller size, and broader relative bandwidth; the DGS need to be optimized to have better effectiveness of reflection within operation frequency 1.7–2.7 GHz. As shown in Figure 1(a), the proposed DGS structure is printed on the bottom of dielectric

substrate. It has a complete symmetry around the geometric center and has a reflection phase from -90 to 90 degrees within operation frequency to cover broadband detection requirements. In this design, the DGS structure is composed of a central reflection region and an edge reflection region. The gap of the edge reflection region is located at the bottom of the antenna radiating elements to enhance antenna radiating performance. One coaxial feed line runs through the entire structure from antenna to DGS. The external of coaxial feed line is connected to DGS. The coaxial line will feed antenna radiating element. Figure 1(b) is the antenna radiating element.

While having wider operation band and higher antenna gain, for the robot positioning system requirements, the design of miniaturization antenna is pursued in two aspects: antenna radiating element and reflection element. Here, the radiating elements involve the radiating element arm, feeding sheet, and transmission line. Based on this, four radiating elements are printed on a dielectric substrate, with an angle of 90 degrees to each adjacent element. To expand antenna impedance bandwidth and improve the antenna gain, the sizes of the four radiating elements of the antenna are different and optimized to meet four individual quarter wavelengths continuously from 1.7 to 2.7 GHz. The geometric parameters of the antenna structure are shown in Table 1.

3. Modeling and Simulation

As mentioned above, we studied a compact broadband robot positioning antenna unit, consisting of a radiation sheet, DGS structure, and feed cable. The proposed structure has been modeled and simulated by using commercial simulation software (CST), and the simulation results are shown in

TABLE 1: Geometric parameters of the antenna and its DGS structure (mm).

Label	Size
L1	6
L2	3.6
L3	1.1
L4	8
L5	4
L6	5
L7	14
L8	8.2
L9	7
L10	8.2
L11	6
L12	31
L13	17
L14	17.5
L15	6
L16	11
L17	4.6
LA1	2
LA2	7
LA3	3
LA4	8.2
LA5	29.2
LA6	17.5
LA7	12
LA8	8.2
LA9	11
LA10	12.5
LA11	4
LB1	7.8
LB2	8.5
LB3	20
LB4	11
LB5	6.5
LB6	2
LB7	5.1
LB8	3
LB9	17
LB10	5
LB11	9
LB12	9.5
LC1	27
LC2	8
LC3	6
LC4	6.5
LC5	2
LC6	7.5
LC7	14
LC8	12

TABLE 1: Continued.

Label	Size
LC9	14
LD1	3.5
LD2	9.5
LD3	25
LD4	13
LD5	4
LD6	5
LD7	2.3
LD8	9.5
LD9	8

Figure 2, that is, antenna unit S-parameter in Figure 2(a) and radiation pattern of the antenna unit in Figure 2(b). The S-parameters are simulated within 1–3 GHz. The simulated result indicates that the return loss ($|S_{11}|$) of the antenna unit is less than -10 dB within the operating frequency. Also, the radiation gain of the antenna unit is greater than 2 dB.

In order to verify the practicality and reduce the size of the proposed DGS antenna, we employ a couple of units to build one antenna array. Taking the extreme case as an example, the interval between two antenna units is 0 cm and cophase feeding with constant amplitude is conducted on a dual-element antenna, as shown in Figure 3. To test the performance of the antenna unit in various circumstances, the phase angle of the dual-element antenna unit is, respectively, set to 0° , 90° , 180° , or 270° .

The simulated results of the S-parameters are shown in Figure 4. $|S_{11}|$ and $|S_{22}|$ are the return losses of two ports, and $|S_{21}|$ is the isolation between the two ports. As shown in Figure 4, all simulated $|S_{11}|$ and $|S_{22}|$ are below -10 dB within working frequency 1.2–2.7 GHz, while the simulated $|S_{21}|$ is below -20 dB, indicating that the designed antenna units have good impedance bandwidth characteristics and a good isolation between the two units because of the adopted DGS reflection technology. Even the interval between two antenna elements is 0 cm, this greatly improves the adaptability of the antenna unit and enables them to be intensively arranged without affecting antenna performance, which greatly reduces the geometric size of the antenna array suitable for a robot positioning system. Through different arrangements and increasing or decreasing the number of antennas, the antenna system can achieve the desired performance of the antenna positioning system.

At the frequency of 2 GHz, the simulated far-field radiation pattern of the positioning antenna array at the H -plane is shown in Figure 5. Because the four radiating elements of one antenna unit are not identical, to further validate the performance of the antenna unit in an array, the phase difference of the dual-element antenna unit is set as 0° , 90° , 180° , or 270° . The simulation results present the maximum gain of the antenna greater than 4.67 dB, and the width of the main lobe beam is 56 – 68° . The result shows that the antenna radiation

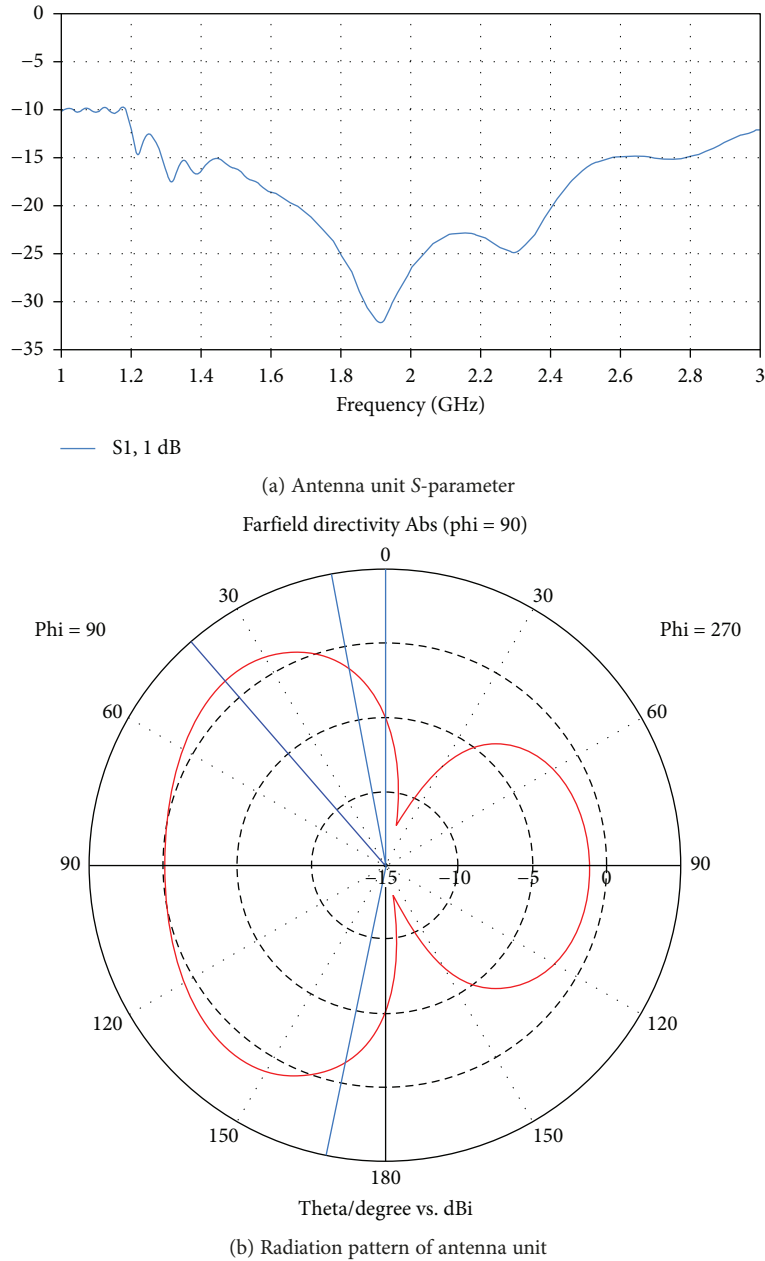


FIGURE 2: Diagram of the S-parameter and radiation pattern.

pattern is consistent, which indicates that the radiation performance of the designed positioning antenna is stable. The above simulation test results show that the proposed antenna design has a small size, wide-frequency band, high isolation, and stable radiation performance, which are suitable for small-sized robot positioning antenna system.

To further verify the proposed antenna, based on the above simulation results, we employed four elements to build an antenna array. As shown in Figure 6, four antenna units are placed in a plane with an antenna element spacing of 0 mm and 0 degree phase angle between adjacent elements. The simulated S-parameter results are presented in Figure 7. Within the operation frequency 1.7–2.7 GHz, the return loss of antenna elements ($|S_{11}|$, $|S_{22}|$, $|S_{33}|$, and $|S_{44}|$) is all below -10 dB and the mutual coupling ($|S_{14}|$,

$|S_{23}|$) between any two antenna elements is lower than -20 dB, which means good isolation between any two antenna elements. Also, the far-field pattern of the four-element antenna is shown in Figure 8. The radiation pattern of the antenna system at 2 GHz is greater than 8 dB and points to different directions, which meets the requirement of a robot positioning system antenna for high-precision positioning purpose.

4. Measurement

A prototype of the configuration employing the DGS has been fabricated in order to experimentally validate the proposed design, as shown in Figure 9. The measured S-parameters are also presented in Figure 10 for comparison.

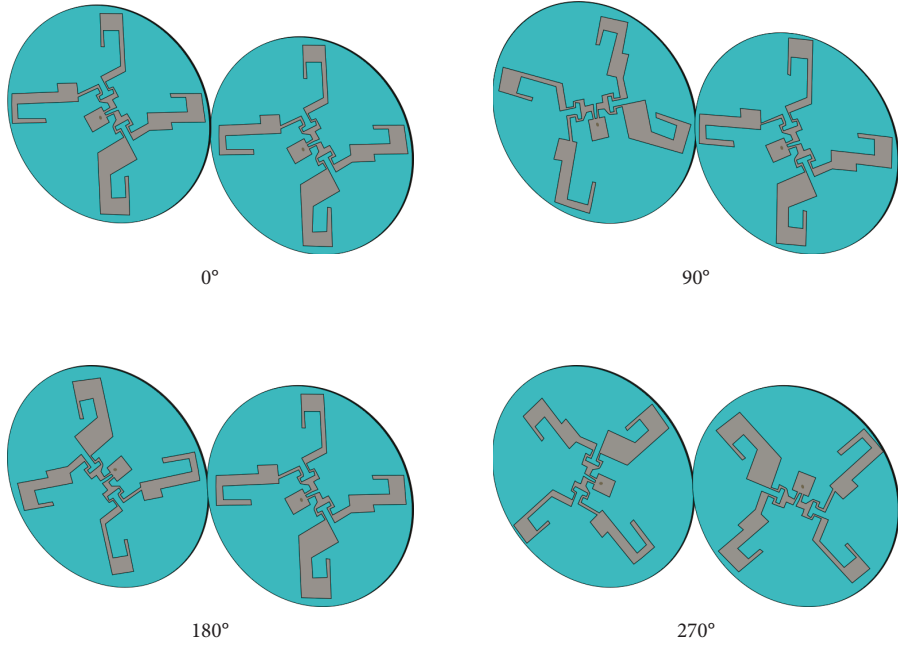


FIGURE 3: Schematic diagram of the dual-element antenna array.

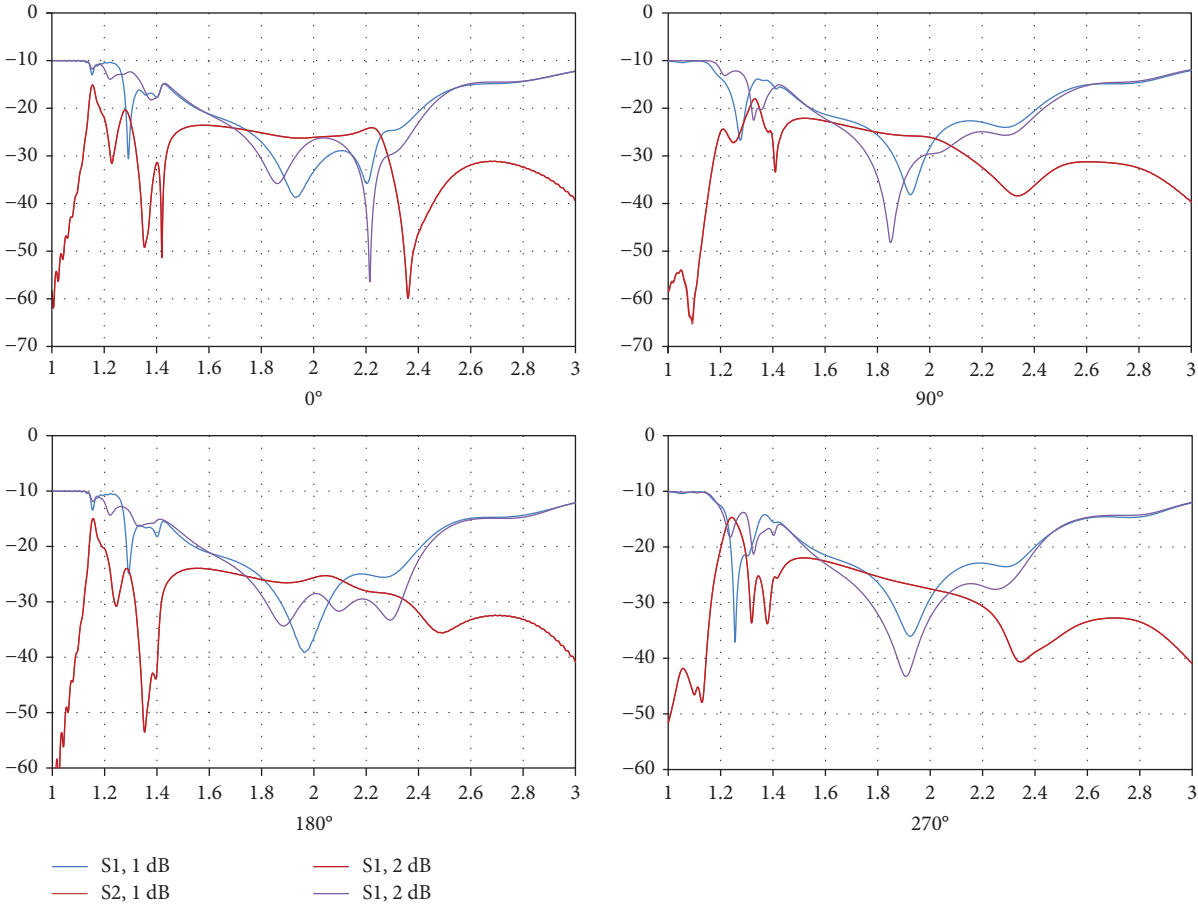


FIGURE 4: Simulation of S-parameters of dual-element antenna array structure.

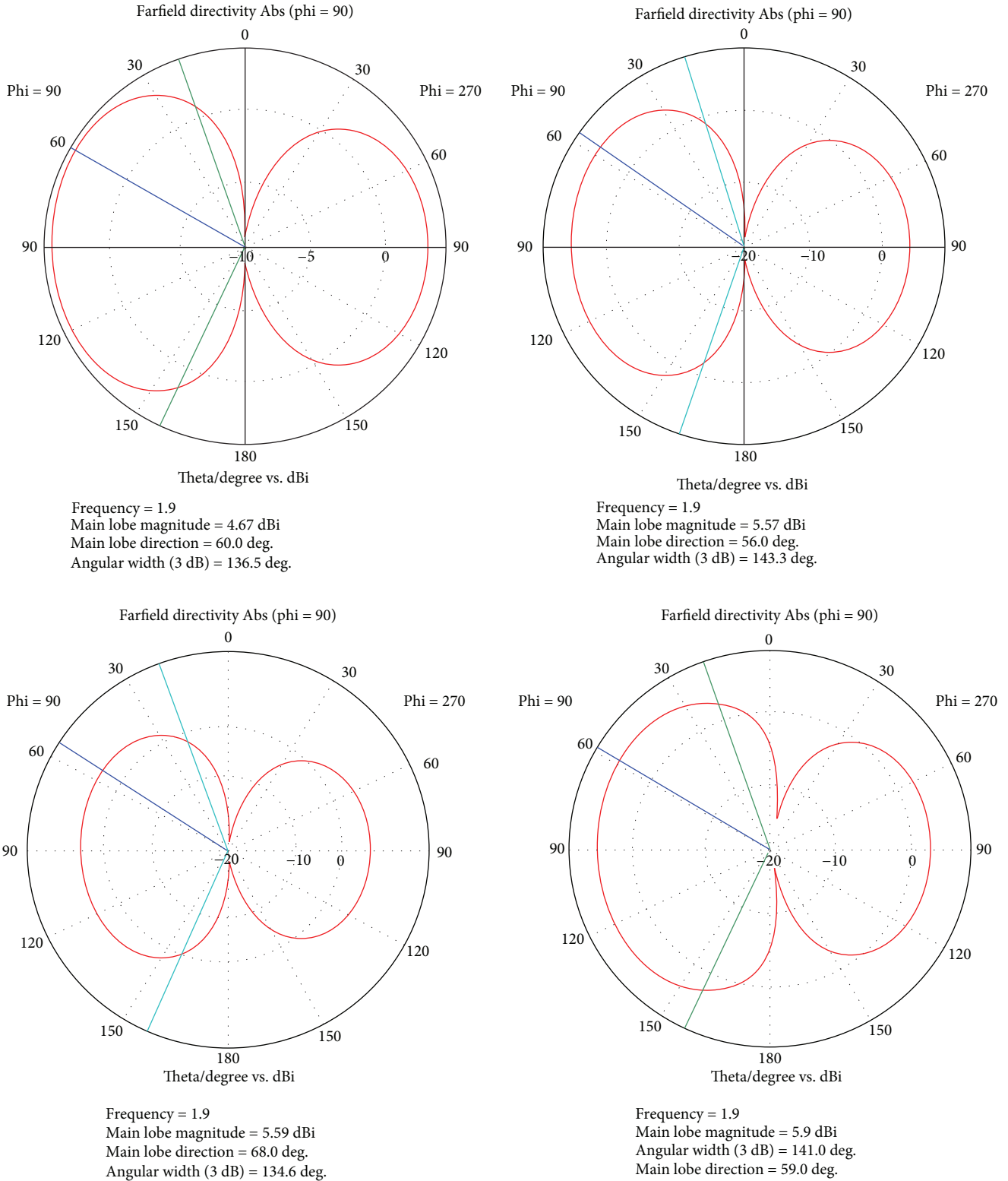


FIGURE 5: Simulation radiation pattern of dual-element antenna array structure.

These results validate that, in the presence of the DGS, the antenna operates within the desired frequency ($S_{11} < -10$ dB). The resonances of measurement result are very slightly shifted. These minor discrepancies are due to fabrication imperfections in the manual soldering of the

feeding and shorting pins of the antenna. The antenna radiation pattern has been assessed experimentally. It is matching the simulation results; the radiation gain of antenna unit is greater than 2 dB, as presented in Figure 11. The measured results match the simulation presented above.

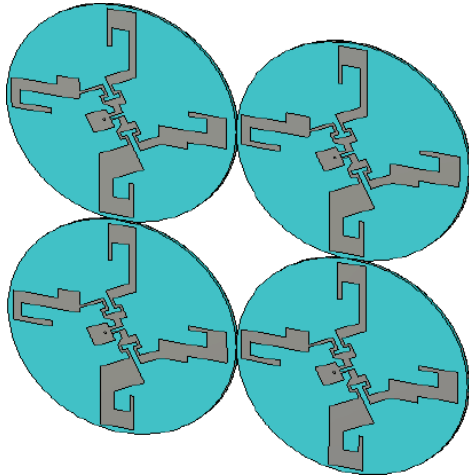


FIGURE 6: Schematic diagram of a four-antenna array structure.

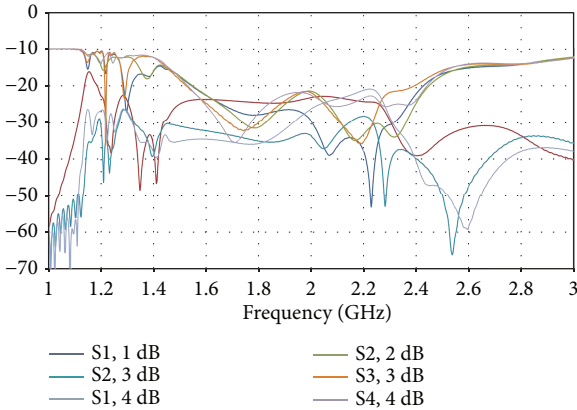


FIGURE 7: S-parameter simulation of a four-antenna array structure.

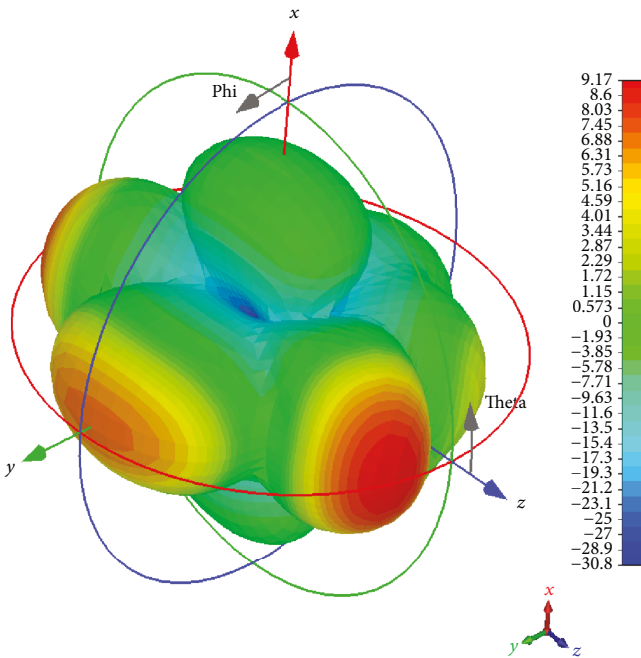


FIGURE 8: Far-field pattern of a four-antenna array structure.



FIGURE 9: Prototype of the antenna system using the proposed DGS.

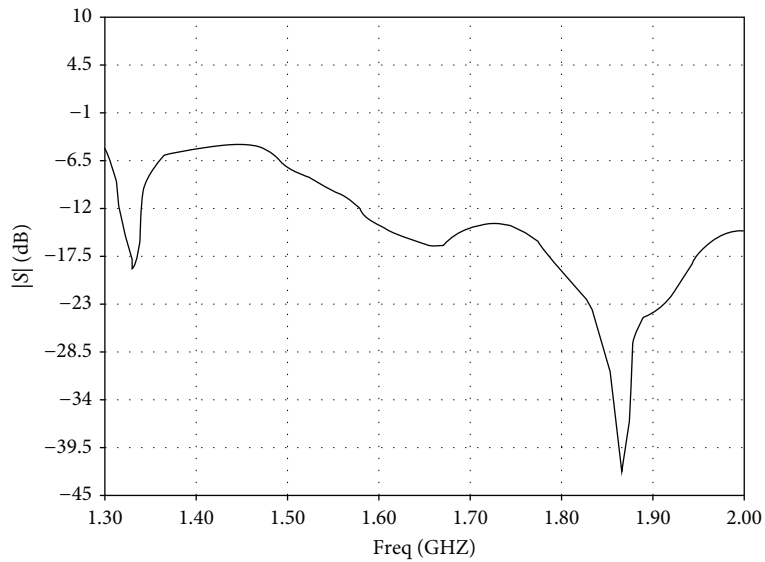


FIGURE 10: Measured S-parameters for a single unit.

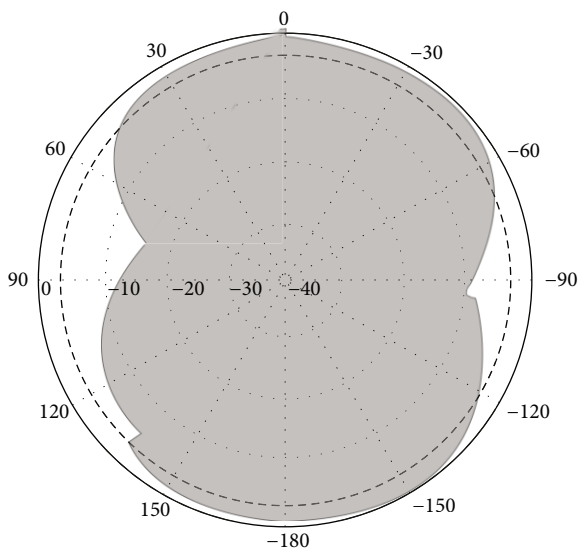


FIGURE 11: Measured radiation pattern (gain) of one antenna unit ($|S|$, dB).

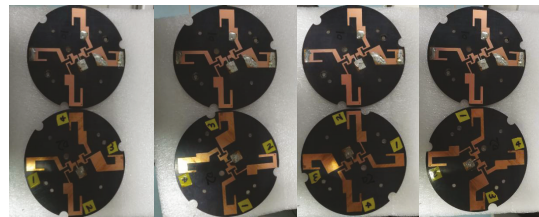


FIGURE 12: The experimental model of the dual-element antenna array.

Based on the configuration and dimensions of the single antenna element, a dual-element antenna array is also studied. A configuration and an experimental prototype of the proposed antenna system are shown in Figure 12. The interval between two antenna units is 0 cm; cophase feeding with constant amplitude is conducted on a dual-element antenna. The phase angle of the dual-element antenna unit is, respectively, set to 0° , 90° , 180° , or 270° . After fabrication, the measurement results have been presented in Figure 13. All measured antenna return loss ($|S_{11}|$, $|S_{22}|$) is below -10 dB, while the measured mutual coupling $|S_{21}|$ is below -20 dB, indicating that the designed antenna units have

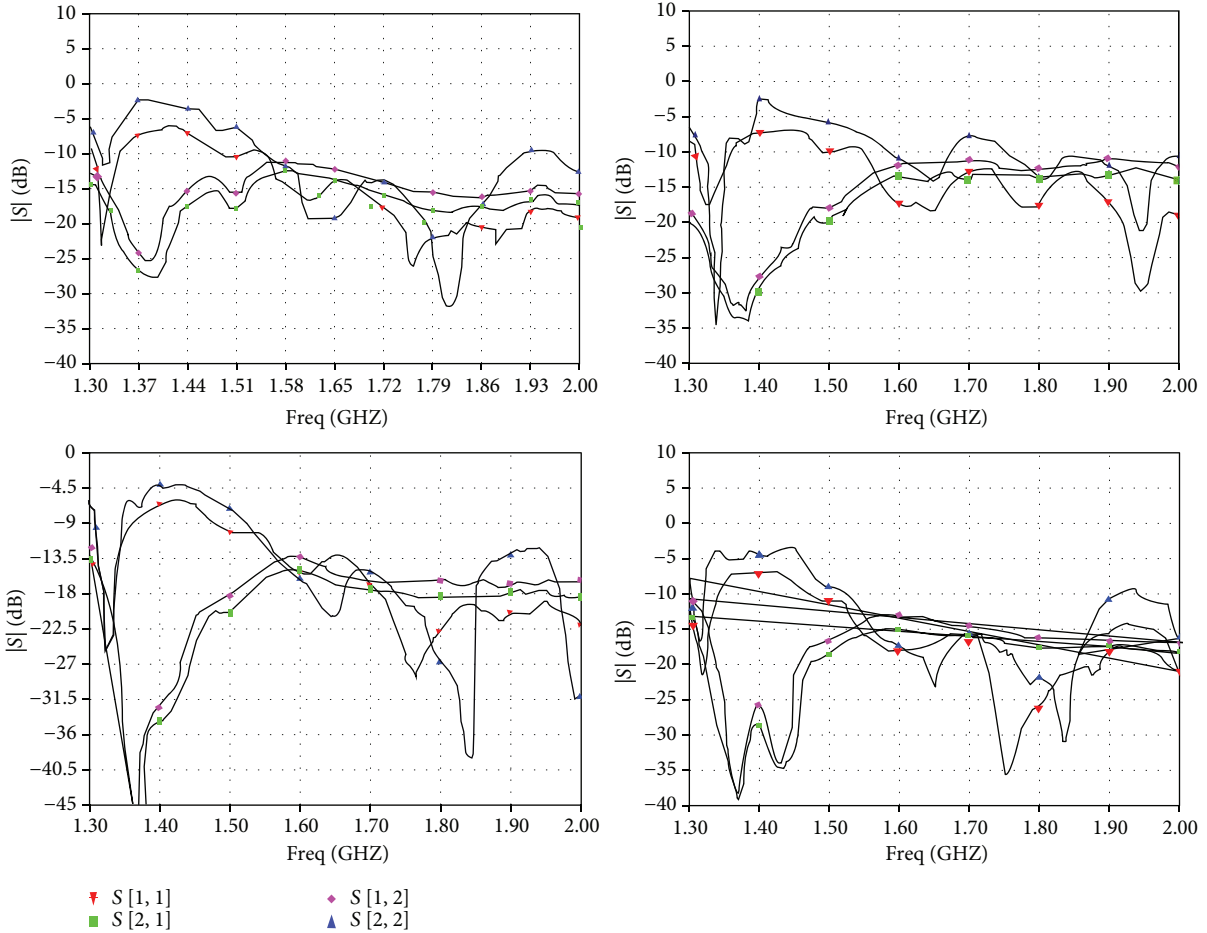


FIGURE 13: Measured S-parameters of the dual-element antenna array.

good impedance bandwidth characteristics and a good isolation between the two antenna elements. Also, the antenna radiation pattern has been measured experimentally. It is matching the simulation results; the radiation gain of two antenna elements is greater than 3 dB. And, they are very similar as presented in Figure 14.

5. Conclusion

As presented above, one DGS-based wide-band robot positioning antenna and an array have been proposed. The antenna unit is primarily composed of four parts, i.e., optimized printed radiating sheet, periodic DGS structure, coaxial feed line, and supporting substrate. The printed radiating sheet has been separately optimized that enables the return loss of antenna to be lower than -10 dB and the far-field gain over 2 dB within the operation frequency range from 1.7 to 2.7 GHz. To test the performance of the antenna design, the spacing of two antenna elements is set at 0 mm and the phase angle separately as 0° , 90° , 180° , or 270° . Simulated result as well as measurements of fabricated prototypes presented that the proposed antenna array has good impedance bandwidth characteristics. Also, the maximum antenna gain exceeds 4.67 dB, with an essentially consistent radiating pattern, which indicates that the radiating performance of the robot

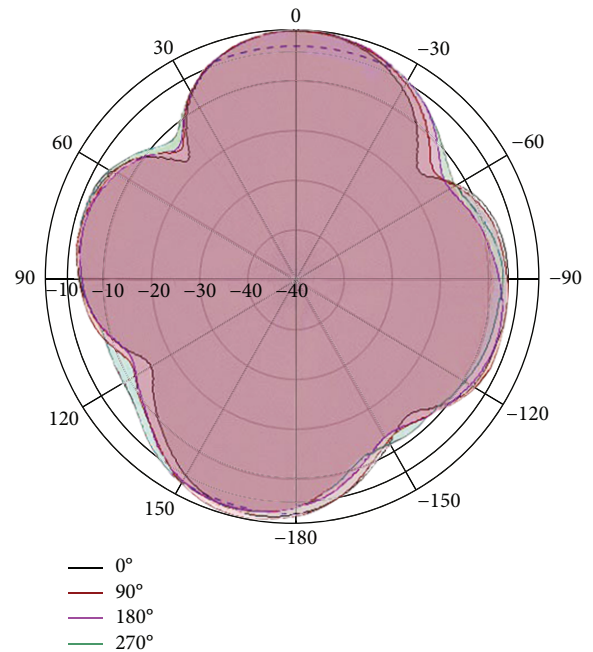


FIGURE 14: Measured radiation pattern (gain) of the dual-element antenna array ($|S|$, dB).

positioning antenna array designed in this study is stable. Lastly, the simulation results show that the positioning antenna system consisting of quad-element units can operate in the entire working frequency range of 1.7–2.7 GHz while providing an antenna gain of more than 8 dB, having good directionality. In short, the proposed small-sized positioning antenna in this study is simple in design, easy to combine, and with good performance and achieves one compact antenna-feed system. Thus, the proposed structure is suitable for compact robots.

Data Availability

The data used to support the findings of this study are available from the corresponding author upon request.

Conflicts of Interest

The authors declare no conflict of interest.

References

- [1] W. Weihua, *Research on Positioning Technology of Mobile Robot*, Huazhong University of Science and Technology, Wuhan, 2005.
- [2] N. Guochen, X. Ping, and F. Qi, "Self-localization of mobile robot based on odometer and PTZ vision," *Computer Application*, vol. 31, no. 10, pp. 2821–2824, 2011.
- [3] X. Daisheng, H. Zhiping, S. Rong, and W. Jianyu, "Optical design of laser guided target azimuth detection system," *Optics & Optoelectronic Technology*, vol. 2, no. 5, pp. 1–4, 2004.
- [4] L. Shaoping, *Research on AGV Positioning and Guidance Based on RFID*, Shandong University, Ji Nan, 2011.
- [5] B. Hongrui, L. Feng, L. Feng, and W. Donglai, "Attitude control of four rotor aircraft based on UM6 inertial navigation module," *Computer & Digital Engineering*, vol. 8, pp. 18–21, 2012.
- [6] L. Kinde, H. Xinhan, and M. I. N. Wang, "Sonar grid map creation based on classic DSMT," *Application Research of Computers*, vol. 3, pp. 209–212, 2007.
- [7] L. Bing, *Research on the Miniaturization of Broadband Base Station Antenna*, University of Electronic Science and Technology, Cheng Du, 2013.
- [8] W. Maowen, Z. Heng, and G. Baoping, "A novel broadband dual polarized base station antenna," *Modern Radar*, vol. 36, no. 4, pp. 56–60, 2014.
- [9] B. G. Duffley, G. A. Morin, M. Mikavica, and Y. M. M. Antar, "A wide-band printed double-sided dipole array," *IEEE Transactions on Antennas and Propagation*, vol. 52, no. 2, pp. 628–631, 2004.
- [10] T. Laohapensaeng and K. Boonying, "Dual polarized microstrip antenna with high isolation using an inserted slot," in *2011 International Symposium on Intelligent Signal Processing and Communications Systems (ISPACS)*, pp. 1–5, Chiang Mai, Thailand, December 2011.
- [11] F. H. Yang and W. Tang, "A novel low-profile high-gain antenna based on artificial magnetic conductor for LTE applications," in *ISAPE2012*, pp. 171–174, Xian, China, October 2012.
- [12] S. Best and D. Hanna, "Design of a broadband dipole in close proximity to an EBG ground plane," *IEEE Antennas & Propagation Magazine*, vol. 50, no. 6, pp. 52–64, 2008.
- [13] C. Insik and L. Bomson, "Design of defected ground structures for harmonic control of active microstrip antenna," in *IEEE Antennas and Propagation Society International Symposium (IEEE Cat. No.02CH37313)*, pp. 852–855, San Antonio, TX, USA, June 2002.
- [14] J.-S. Park, J.-H. Kim, J.-H. Lee, S.-H. Kim, and S.-H. Myung, "A novel equivalent circuit and modeling method for defected ground structure and its application to optimization of a DGS lowpass filter," in *2002 IEEE MTT-S International Microwave Symposium Digest (Cat. No.02CH37278)*, pp. 417–420, Seattle, WA, USA, June 2002.
- [15] G.-L. Wu, W. Mu, X. W. Dai, and Y. C. Jiao, "Design of novel dual-band bandpass filter with microstrip meander-loop resonator and CSRR DGS," *Progress in Electromagnetics Research*, vol. 78, pp. 17–24, 2008.
- [16] L. H. Weng, Y. C. Guo, X. W. Shi, and X. Q. Chen, "An overview on defected ground structure," *Progress in Electromagnetics Research B*, vol. 7, pp. 173–189, 2008.
- [17] T. Kokkinos, E. Liakou, and A. P. Feresidis, "Decoupling antenna elements of PIFA arrays on handheld devices," *Electronics Letters*, vol. 44, no. 25, pp. 1442–1444, 2008.
- [18] Q. Li, A. P. Feresidis, M. Mavridou, and P. S. Hall, "Miniaturized double-layer EBG structures for broadband mutual coupling reduction between UWB monopoles," *IEEE Transactions on Antennas and Propagation*, vol. 63, no. 3, pp. 1168–1171, 2015.

